AJNR

Potential of T2 relaxation time measurements for early detection of radiation injury to the brain: experimental study in pigs.

E Miot-Noirault, S Akoka, D Hoffschir, D Pontvert, G Gaboriaud, C Alapetite, F Fetissof and A Le Pape

AJNR Am J Neuroradiol 1996, 17 (5) 907-912
http://www.ajnr.org/content/17/5/907

Potential of T2 Relaxation Time Measurements for Early Detection of Radiation Injury to the Brain: Experimental Study in Pigs

E. Miot-Noirault, S. Akoka, D. Hoffschir, D. Pontvert, G. Gaboriaud, C. Alapetite, F. Fetissof, and A. Le Pape

PURPOSE: To investigate the MR T2 relaxation time and histologic changes after a single-fraction 25-Gy dose of radiation to the brain of pigs. **METHODS:** The right hemisphere of 10 Meishan pigs was irradiated with a single dose of 25 Gy at the 90% isodose, using a 12-MeV electron beam. T2 relaxation time was measured within three regions of interest in the brain: those that had received 90%, 70%, and 40% of the total dose, respectively. T2 kinetics over time was compared with histologic studies. **RESULTS:** Brain T2 values were noted to increase within the irradiated areas. T2 kinetics were analyzed in three phases: an immediate transient phase and two long-lasting phases. These two long-lasting phases were correlated with the detection of ventricular compression and necrosis, respectively. The T2 increase within the 90% region of interest was 19%, 22%, and 26% for phases I, II, and III, respectively. T2 measurements within other regions of interest were not significant. **CONCLUSION:** Although our results suggest a dose threshold for T2 variations, brain T2 values increased after irradiation at a level at which disease could not be seen on conventional MR images. This illustrates the value of using conventional MR imaging in a quantitative manner to assess molecular tissue abnormalities at earlier stages of developing diseases.

Index terms: Animal studies; Radiation, injuries; Brain, magnetic resonance; Magnetic resonance, tissue characterization

AJNR Am J Neuroradiol 17:907–912, May 1996

Magnetic resonance (MR) imaging has been used for noninvasive investigation of the effects of radiation therapy for many years. The majority of investigations have been anatomic. Contrast on MR images is essentially determined by the contributions from relaxation times and proton density. The differences in signal intensity attributed to abnormalities on MR images result from nuclear MR parameter alterations induced by a variety of histologic, pathologic, and physiological factors. The application of nuclear MR relaxation time measurements to the diagnosis of pathologic processes has been well documented (1–4). Relaxation times are sensitive to changes in the interaction between water molecules and disturbed tissue macromolecules in vivo at the initial stage of a developing pathologic or physiologic process. Measurements of relaxation times provide a direct assessment of the molecular disturbances from which lesions develop. Quantitative MR imaging offers opportunities to establish diagnoses at earlier stages of disease development.

The application of nuclear MR relaxation time as a noninvasive technique to monitor tumoral and normal tissue responses to radiation therapy has been well documented (1, 5–8). Time course analyses of relaxation times in conjunction with histopathologic studies make possible a better understanding of the mechanisms involved in the observed T2 changes in pathologic tissues. Previous follow-up studies of T2 relaxation time within normal brain tissue after radiation injury found that T2 values increased within the irradiated areas (8). T2 kinetics were found to differentiate the acute stage from the

Received May 19, 1995; accepted after revision November 3.

Supported by grant 6120 from the Association pour la Recherche sur le Cancer.

From the Laboratoire de Biophysique Cellulaire et RMN, Tours (E.M-N., S.A., A.L.P.), CEA/DSV, Bruyères Le Chatel (D.H.), Institut Curie, Paris (D.P., G.G., C.A.), and Laboratoire d'Anatomo-Pathologie, Tours, (F.F.), France.

Address reprint requests to Dr Elisabeth Miot-Noirault, Laboratoire de Biophysique Cellulaire et RMN, Inserm U316-2bis, bd Tonnellé, 37032 Tours Cédex France.

AJNR 17:907–912, May 1996 0195-6108/96/1705–0907

later stage of edema and necrosis. For the higher single doses investigated (ie, 40 Gy and 60 Gy), an increase in the T2 value was dose-dependent for rapidity of onset and severity. The previously described dose dependence of relaxation time changes is particularly fascinating.

The purpose of this work was to investigate the changes in T2 relaxation time and their histopathologic correlation after a low dose (ie, 25 Gy) of radiation in order to study the relationship between brain T2 kinetics and dose dependence after a typical radiation dose as used in conventional radiation therapy.

Materials and Methods

Animal Model

The Meishan pig was used as the animal model for this study. All animals were kept in an animal housing facility, fed pig chow, and given water ad libitum. The facilities and practices were in accordance with European guidelines for experimentation on animals.

All animals were anesthetized with 25 mg/kg pentobarbital sodium intraperitoneally and 3 mg/kg xylazine hydrochloride intramuscularly for the irradiation procedure. Pigs were placed in a prone position and the electron beam port was positioned over the dorsal surface of the right hemisphere. A 40 × 35-mm port was used for beam delivery to the right hemisphere. Pigs were irradiated with a 12-MeV electron beam at a rate of 2 Gy/min. The skin surface dose was calculated to obtain an average brain dose at a depth of 2 cm (90% isodose). Ten animals received a single dose of 25 Gy at the 90% isodose.

MR Imaging

In vivo MR imaging was performed on anesthetized animals using a 2.35-T proton imaging system. Examinations were conducted using a 20-cm bird cage resonator. At the beginning of each experiment, sagittal locater images were acquired to facilitate a reproducible localization of the coronal sections from the cerebellum to the olfactory bulbs of the animals.

Spin-echo T2-weighted coronal imaging was performed using parameters of 3000/30, 60, 90, 120, 150, 180/1 (repetition time/echo time/excitations). All images were obtained using a 256 × 256 matrix and a 20-cm field of view, resulting in a 780-μm pixel size. Each coronal section was 5 mm thick with 2.5-mm intersection spacing. Ten coronal sections were obtained. The examination took about 40 minutes.

Qualitative analyses of the MR images were done to detect general morphologic abnormalities. Quantitative measurement of T2 values was made using techniques described previously (9–11). Three selected regions of interest (ROIs) were placed within each of the irradiated and contralateral hemispheres. Each of these three regions had received different doses from the beam: the first at the 90% isodose (region A), the second at the 70% isodose (region B), and the third at the 40% isodose (region C) (Fig 1). ROIs were represented by a circle of three pixels in minimum diameter, corresponding to a surface of approximatively 4 mm^2. An ROI chosen in the nonirradiated cheek muscle was used as an internal control to normalize any variation in our technique for measuring relaxation time. For each ROI, a T2 ratio, *R,* was calculated: *R* = T2 after irradiation/T2 before irradiation. *R* values were averaged for the 10 animals. Curves of average T2 ratios were plotted as a function of time after radiation therapy for each ROI. MR studies were performed before radiation treatment, every 2 days during the 15 days after treatment, and then at weekly intervals.

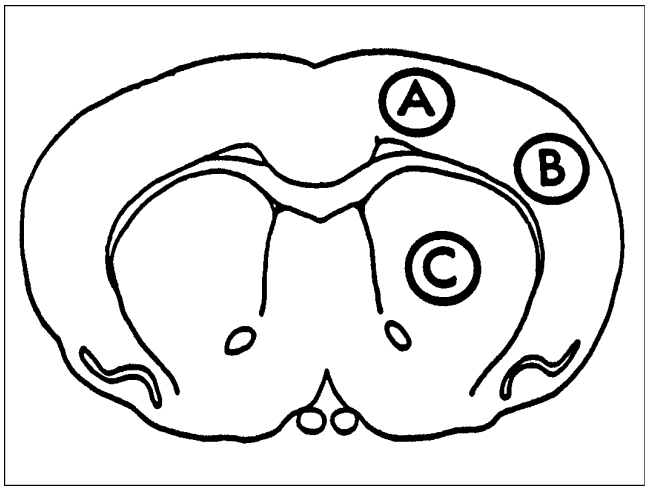

Fig 1. Regions of interest of the coronal brain section studies with T2 relaxation time measurements.

Histology

Histologic examination was performed on pig brains at 2, 9, 25, and 50 days (one animal for each time point), and at 125, 145, and 170 days (two animals for each time point) after irradiation.

Evans blue (7 mL/kg) 2% solution in 9% saline (12) was infused into jugular veins 24 hours before the animal was killed and the brain removed. The pigs received a lethal overdose of sodium pentobarbital and were infused with 10% formalin to ensure uniform fixation. The brains were removed and placed in formalin before being blocked for histologic sectioning and staining. All the brains were then embedded in paraffin and 5-μm coronal sections were cut from the cerebellum to the olfactory bulbs. Selected regions corresponding to the coronal MR sections were stained using hematoxylin-eosin and Luxol fast blue to detect general morphologic abnormalities and regions of demyelination and axonal injury. Microscopic specimens were evaluated for sites of tissue necrosis, demyelination, vessel wall thickening, gliosis, calcification, and hemorrhage. Alterations in the blood-brain barrier were targeted by the Evans blue coloration on each side of the brain.

Results

MR Imaging

Quantitative Analysis: Relaxation Times.—The standard deviation for T2 measurement was 5%. We observed three different T2 phenomena within the irradiated areas: a transient early spike (phase I), an initial prolonged T2 increase (phase II), and a second prolonged T2 increase (phase III). Figure 2A shows the *R* curve of the 90% isodose and equivalent contralateral ROI. (For better legibility, error bars are not plotted; in these cases, the interindividual variation was 15%.)

Following the transient phase I (19% increase), at 2 days after irradiation, we observed the first long-lasting (22%) increase in the *R* curve (phase II) from the 30th day to the 110th day after irradiation. Phase III began on the 130th day after treatment (26% increase) and completed the curve with another increase of *R* up to 40% at day 170.

T2 ratio kinetics could be split in two long-lasting phases (phase II and phase III). Ventricular compression was seen early, but after phase II. Hyperintense T2 parenchymal changes were visible on the MR images only after the onset of phase III. Figure 2B and 2C shows R curves for the 70% and 40% isodoses, respectively, and equivalent contralateral ROIs. In phase II, we observed 18% and 13% T2 increases within the 70% and 40% isodose ROIs, respectively. In phase III, the *R* value increased 18% and 10% within regions B and C, respectively. The average *R* curves for the 70% and 40% isodose irradiated ROIs (regions *B* and *C,* respectively) were not significantly different from the *R* average curve of the contralateral nonirradiated ROI (interindividual variation was about 15%). For the doses investigated (ie, 19 Gy and 11 Gy for regions B and C, respectively), the slightly higher *R* values did not seem to be proportional to the actual dose received. The timing of this phenomenon was dependent on the maximal dose received (90% isodose).

Qualitative Studies.—The first visible radiation-induced anatomic MR change was compression and occlusion of the irradiated lateral ventricle. This appeared in the irradiated hemisphere on T2-weighted images after phase II at day 110 (±10) after irradiation. This change was seen in only 50% of the irradiated animals.

The second radiation-induced anatomic MR change was characterized by a visible increase

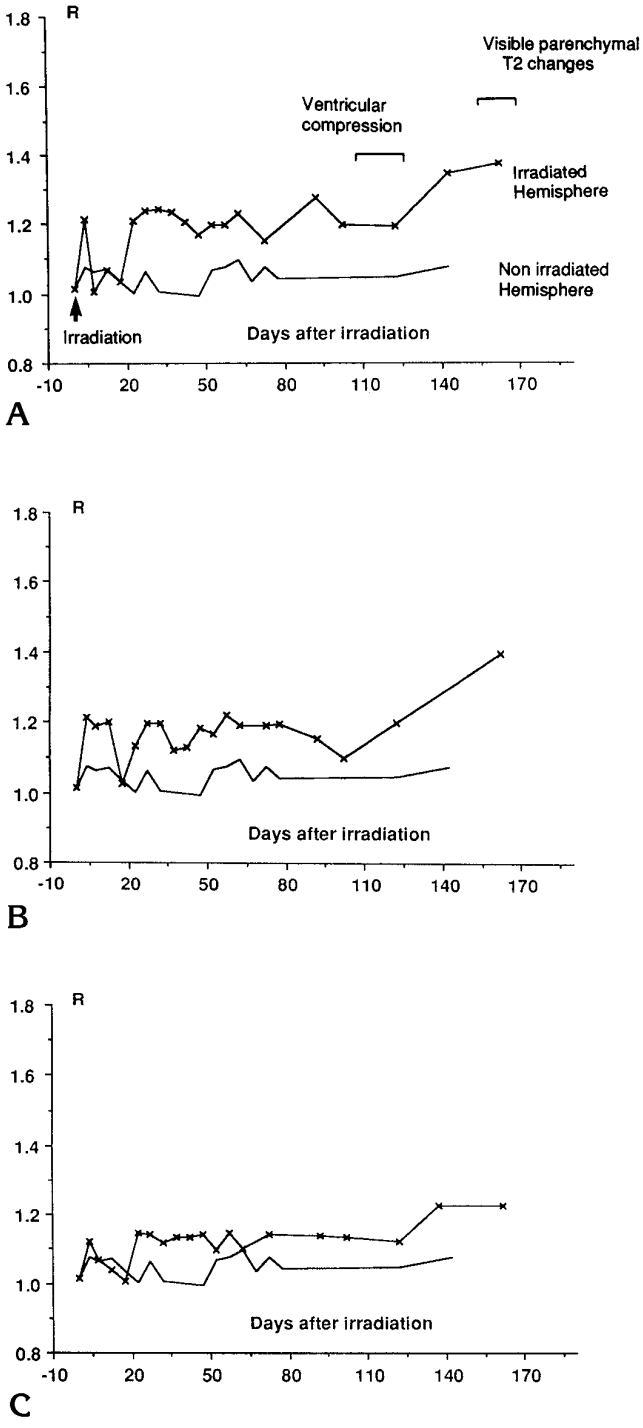

Fig 2. *R* curves of irradiated and contralateral regions of interest (ROI) of the pig brain as a function of time after radiation therapy with a dose of 25 Gy (12 MeV, electron beam). (To increase readability, errors bars were not plotted; in these cases, the interindividual variations were 15%). *Hatched line* indicates the irradiated ROI; *smooth line* indicates the contralateral ROI.

A, Curve of 90% isodose ROI (region A).

B, Curve of 70% isodose ROI (region B).

C, curve of 40% isodose ROI (region C).

Fig 3. Coronal T2-weighted MR image of a pig brain 170 days after irradiation with 25 Gy (12 MeV, electron beam). Note increased signal intensity in the periventricular gray and white matter (*arrows*), suggesting the presence of necrosis.

in the signal intensity of the periventricular gray and white matter on T2-weighted images. This appeared in the irradiated hemisphere on T2-weighted images after phase III at day 170 (±10) after irradiation (Fig 3). This change was seen in all the pigs that survived beyond this date. This visible signal change was correlated with the detection of necrosis on the corresponding histologic sections.

Histology

Inflammation of the meninges was observed 2 days after irradiation. A discrete macrophage inflammation in the periventricular region and choroid plexus appeared on histologic sections 9 days after irradiation. Vascular congestion could also be observed. The inflammation process was observed to spread through the parenchymal tissue of brain excised 25 days after irradiation. At 50 days after irradiation, we observed a considerable inflammatory process and a vascular and glial injury, possibly leading to transient edema located in the periventricular regions. At 125 days after irradiation, there were no important parenchymal lesions, although there were still inflammatory lesions in the periventricular regions. Congested vessels were noted also. Early necrosis restricted to the periventricular areas was observed at 145 days after irradiation. At 170 days after irradiation, large areas of necrosis were detected in the regions of intense signal on T2-weighted images (ie, in the periventricular regions and in the thalamus). No significant edematous lesions were observed. There was considerable disorganization of nerve tissue, and intracellular calcifications were observed around the necrotic regions. Some lymphocytes were detected around cellular calcifications. Hemorrhagic lesions were seen in the cortex, thalamus, ventricular wall, and meninges.

Evans blue stain appeared to penetrate into the irradiated hemisphere 170 days after irradiation. At this later stage, the Luxol fast blue coloration was very low in the irradiated hemisphere; myelin fibers were also disorganized.

Discussion

We followed the 6-month course of T2 relaxation time and histologic changes in brain tissue after a single-fraction 25-Gy dose of radiation to part of the right hemisphere in a pig brain. Our studies produced the following observations: A single-fraction 25-Gy dose of radiation induces an increase in the T2 relaxation time within brain tissue. The three phases of increased T2 described previously (8) were observed within the 90% isodose ROI: a transient spike (phase I), an initial and prolonged T2 increase (phase II), and a second prolonged T2 increase (phase III).

The dose dependence of increased T2 relaxation time after a 25-Gy dose of radiation was also observed, but was less obvious: T2 increased 19%, 22%, and 40% for phases I, II, III, respectively, within the 90% isodose ROI; T2 kinetics showed no significant differences between the contralateral nonirradiated ROIs and the 70% and 40% isodose ROIs (ie, 19 Gy and 11 Gy, respectively). This correlates well with previous findings (8): the T2 curve within a 40% isodose ROI of a 40-Gy group (ie, 17 Gy) was not significantly different from the T2 curve within the contralateral ROI. Our results suggest a dose threshold for the sensitivity of our quantitative MR imaging technique of around 20 Gy. The T2 increase rate (at a 70% and 40% isodose) was around 18%. However, because of a 15% interindividual variation, this difference was not statistically significantly different from the T2 kinetics in contralateral regions.

Consistent results were found between MR imaging and histologic studies: the transient spike (phase I) seems to be related to a transient, discrete inflammatory process. At this stage, no abnormalities could be seen on T2-

weighted images. Compression of the irradiated ventricle starts after the onset of phase II. Nevertheless, this anomaly was observed in only 50% of the animals. These results agree with those obtained in clinical situations: authors found that qualitative MR imaging could underestimate the extent of histologic lesions induced by interstitial brachytherapy (13). Other authors (14, 15) found MR imaging abnormalities in only half the patients examined after an average radiosurgical dose of 38 Gy.

Phase II seemed to be related to a significant inflammatory process and to endothelial damage. At day 125, histologic examination performed on two pig brains revealed congestion in vessels. Investigators who have performed experimental irradiation with single doses of approximatively 25 Gy have suggested a tendency toward venous rather than arterial congestion (16, 17). Our findings in just two brains are too limited to allow speculation as to any such tendency.

Abnormalities were detected after phase III within regions of high signal intensity on T2-weighted images. Necrotic regions were characterized on MR images by an increase in the signal intensity of gray and white matter on T2-weighted images. High signal intensity in the white matter is a generally accepted finding on T2-weighted spin-echo MR images after radiation therapy (18, 19). T2-weighted imaging could not differentiate the signal of necrotic regions from the signal of edema. Both necrosis and edema appear as heterogeneous high signal on T2-weighted images (20). At 170 days after irradiation, histologic analysis revealed necrosis in regions of intense signal on T2-weighted images, with no significant associated edema. This finding may be explained by the time at which histologic examination was performed: 170 days after a 25-Gy dose of radiation is probably too earlier to observe any spread of edema. Researchers who administered a 25-Gy dose of radiation to the brains of rats (17) observed two waves in the development of edema: 13 weeks after irradiation, a transient edema developed and tended to decrease with time; after 6 months, a second wave of severe edema was observed. It has also been suggested that the maximum level of vascular damage in the rat brain seems to be reached 39 weeks after a 25-Gy dose. Others authors (21) have also observed that the latency period of the gross vascular changes associated with edema (44 weeks) was longer than that for necrosis (35 weeks).

In our study, the Luxol fast blue coloration was very low in the irradiated hemisphere at day 170, suggesting that alterations in the blood-brain barrier did not spread. This was also consistent with another study, in which it was found that changes in the permeability of the blood-brain barrier occurred only at 18 months after doses of around 20 Gy (22).

MR imaging has been used for the study of radiation injury since 1985 (1, 2, 4–8, 13–15, 23–25). An increase in relaxation time after irradiation has been reported previously (1, 2, 4–8); however, the highest single doses used in these studies were never under 20 Gy (1, 2, 4–6, 8). A study conducted by Brennan et al (7) on dogs who were given high single doses of 7.5 to 15 Gy showed that no histologic abnormalities were detected on MR images in the dogs who had received doses lower than 13 to 15 Gy.

Although our study introduced a dose threshold for significant T2 variation, this last parameter increase occurred at a stage at which no signal or anatomic abnormalities were apparent on T2-weighted MR images. Indeed, the first radiation-induced anatomic lesion (ie, lateral ventricle compression) was seen only 4 months after treatment and in only 50% of the animals studied. In contrast, the first long-lasting T2 increase (phase II) occurred as early as the first month after treatment and was observed in all animals. Moreover, measurement of T2 relaxation time, which is feasible on most clinical imaging systems, remains an easy method by which to detect disease processes at an early stage of development.

Conclusion

The results reported here illustrate the value and limits of MR T2 relaxation time in assessing radiation-induced changes in molecular tissue early in their course of development.

The advantages of following T2 relaxation time to elucidate the pathophysiology of radiation injury to the brain lies in the ability to follow the pathologic processes over time. The dose threshold of significant changes in T2 values suggest that our experimental model could be useful for patients treated with clinical radiosurgery, where higher single doses are conventionally delivered to a limited volume of tissue. Nevertheless, T2 relaxation time, which is easily

measured with most clinical imaging systems, remains one of the most sensitive MR methods for detecting early complications of radiation therapy by evaluating radiation-induced cellular disorganization at molecular levels.

References

1. Shioya S, Haida M, Fukuzaki M, et al. A 1-year course study of the relaxation times and histology for irradiated rat lungs. *Magn Reson Med* 1990;14:358–368
2. Bloch P, Lenkinski RE, Buhle EL Jr, Hendrix R, Bryer M, McKenna WG. The use of T2 distribution to study tumor extent and heterogeneity in head and neck cancer. *Magn Reson Imaging* 1991;9: 205–211
3. Kirsch SJ, Jacobs RW, Butcher LL, Beatty J. Prolongation of magnetic resonance T2 time in hippocampus of human patients marks the presence and severity of Alzheimer's disease. *Neurosci Lett* 1992;134:187–190
4. Shioya S, Haida M, Ono Y, et al. Tissue characterization of pneumonia and irradiated rat lungs with magnetic resonance relaxation times. *Magn Reson Imaging* 1994;12:799–803
5. Boesiger P, Greiner R, Schoepflin RE, Kann R, Kuenzi U. Tissue characterization of brain tumors during and after pion radiation therapy. *Magn Reson Imaging* 1990;8:491–497
6. Belfi CA, Medendorp SV, Ngo FQH. The response of the KHT sarcoma to radiotherapy as measured by water proton NMR relaxation times: relationships with tumor volume and water content. *Int J Radiat Oncol Biol Phys* 1991;20:497–507
7. Brennan KM, Roos MS, Budinger TF, Higgins RJ, Wong ST, Bristol KS. A study of radiation necrosis and edema in the canine brain using positron emission tomography and magnetic resonance imaging. *Radiat Res* 1993;134:43–53
8. Miot E, Hoffschir D, Alapetite C, et al. Experimental MR study of cerebral radiation injury: quantitative T2 changes over time and histopathologic correlation. *AJNR Am J Neuroradiol* 1995;16: 79–85
9. Kjos BO, Ehman RL, Brant-Zawadzki M, Kelly WM, Norman D, Newton TH. Reproducibility of relaxation times and spin density calculated from routine MR imaging sequences: clinical study of the CNS. *AJNR Am J Neuroradiol* 1985;6:271–276
10. Mc Fall JR, Wehrli FW, Breger RK, Johnson AJ. Methodology for the measurement and analysis of relaxation times in proton imaging. *Magn Reson Imaging* 1987;5:209–220
11. Tofts PS, Du Boulay EPGH. Towards quantitative measurements of relaxation times and other parameters in the brain. *Neuroradiology* 1990;32:407–415
12. Remler MP, Marcussen WH, Tiller-Borsich J. The late effects of radiation on the blood brain barrier. *Int J Radiat Oncol Biol Phys* 1986;12:1965–1969
13. Oppenheimer JH, Levy ML, Sinha V, et al. Radionecrosis secondary to interstitial brachytherapy: correlation of magnetic resonance imaging and histopathology. *Neurosurgery* 1992;31:336–343
14. Altschuler EM, Lunsford LD, Coffey RJ, Bissonette DJ, Flickinger JC. Gamma knife radiosurgery for intracranial arteriovenous malformations in childhood and adolescence. *Pediatr Neurosci* 1989; 15:53–61
15. Guo W, Lindquist C, Karlsson B, Kihlstrom L, Steiner L. Gamma knife surgery of cerebral arteriovenous malformations: serial MR imaging and spectroscopy. *Radiology* 1993;169:305–309
16. Adolfsson R, Gottfries CG, Hassler O, Roos BE, Winblad B. Late effects on rabbit brain morphology and monoamine metabolites produced by ^{60}Co-irradiation. *Acta Radiol Ther Phys Biol* 1976; 15:433–446
17. Calvo W, Hopewell JW, Reinhold HS, Van Den Berg AP, Yeung TK. Dose-dependent and time-dependent changes in the choroid plexus of the irradiated rat brain. *Br J Radiol* 1987;60:1109–1117
18. Tsuruda JS, Kortman KE, Bradley WG, Wheeler DC, Van Dalsem W, Bradley TP. Radiation effects on cerebral white matter: MR evaluation. *AJNR Am J Neuroradiol* 1987;8:431–437
19. Curran WJ, Hecht-Leavitt C, Shut L, Zimerman RA, Nelson DF. Magnetic resonance imaging of cranial radiation lesions. *Int J Radiat Oncol Biol Phys* 1987;13:1093–1098
20. Valk PE, Dillon WP. Diagnostic imaging of central nervous system radiation injury. In: Gutin PH, Leibel SA, Sheline GE eds. *Radiation Injury to the Nervous System*. New York, NY: Raven Press, 1991:211–237
21. Calvo W, Hopewell JW, Reinhold HS, Yeung TK. Time and dose-related changes in the white matter of the rat brain after single doses of X-rays. *Br J Radiol* 1988;61:1043–1052
22. Keyeux A, Ochrymowicz-bemelmans D, Charlier AA. Early and late effect on the blood brain barrier (BBB) permeability and the antipyrine (AP) distribution volumes in the irradiated rat brain. In: Fielden EM, Fowler JF, Hendry JH, Scott D, eds. *Radiation Research (Proceedings of the 8th International Congress of Radiation Research*). London, England: Taylor & Francis, 1987:260
23. Dooms GC, Hecht S, Brant-Zawadzki M, Berthiaume Y, Norman D, Newton TH. Brain radiation lesions: MR imaging. *Radiology* 1986;158:149–155
24. Constine LS, Konski A, Ekholm S, McDonald S, Rubin P. Adverse effects of brain irradiation correlated with MR and CT imaging. *Int J Radiat Oncol Biol Phys* 1988;15:319–330
25. Grossman RI, Hecht-Leavitt CM, Evans SM, et al. Experimental radiation injury: combined MR imaging and spectroscopy. *Radiology* 1988;169:305–309